CORE
Metadata, citation and similar papers at core.ac.uk
Provided by University of Regensburg Publication Server

Nonlinear subgap photoconductivity of polycrystalline silicon

W. Bock
Siemens AG, Zentrale Forschung und Entwicklung, Otto-Hahn-Ring 6, D-8000 München 83, West Germany

W. Prettl
Universität Regensburg, Institut für Angewandte Physik, D-8400 Regensburg, West Germany

(Received 15 February 1988; accepted for publication 11 May 1988)

The photoconductance of polycrystalline silicon films at photon energies smaller than the band gap has been measured as a function of intensity applying a 1.3 μm wavelength semiconductor laser. The observed photosignal increases superlinearly at low intensities and saturates above about 1.5 W/cm^{-2}. This distinct nonlinearity is caused by a significant energy dependence of optical to thermal cross sections of trap states in the band gap. Assuming a three-level-rate equation model, grain boundary trap densities were evaluated.

Polycrystalline silicon (polysilicon) has a widespread application in microelecronic and in optoelectronic devices. Different processing methods for fabrication make polysilicon useful for solar cells,[1] thin-film transistors,[2] or mainly for resistors and interconnections in integrated circuits.[3] Since the work of Seto,[4] it is known that electrical current transport is controlled by grain boundaries, the disordered regions between adjacent grains. The lattice mismatch in these grain boundaries causes a planar array of localized states, being able to capture free carriers. The accumulated charge constitutes an electrostatic barrier, impeding carriers from free motion. The total amount of charge is mainly given by the two-dimensional density of the trap states N_{ss}. Therefore, much work has been done in evaluating N_{ss} for differently processed polysilicon films. The reported results, however, differ considerably. In many works[3-5] a monoenergetic trap level is assumed to model the dc current transport. These models use many unknown parameters and propose more or less complex transport mechanisms like thermionic emission, thermionic field emission, and tunneling processes. Depending on the values chosen for these unknown parameters, in almost any case an agreement between the theory and the experimental results could be achieved. In a great deal of papers a V-shaped density of states was presented. The trap sites were classified as exponentially decaying band tail states, originally from the potential fluctuations due to the spatial distribution of grain boundary defects. For this result, mainly ac-admittance spectroscopy with[6] and without illumination[7] was applied. A pure optical method in comparison to electron spin resonance (ESR) measurements[8] uses optical absorption to determine N_{ss}. In this work the authors found a narrowing of the band gap by band tails to about 1.0 eV and a hill-shaped trap density, centered about 0.65 eV below the conduction-band edge. Beyond different energy dependences of the gap state density, and apart from various types of samples, it can generally be noticed that the reported total amounts of trap density are distinctly smaller if an optical method is applied.

In this work we present a new method to determine the total density of optically excitable trap states in grain boundaries of p-doped polysilicon. For the first time the optical saturation of the photoconductance of thin polysilicon films has been investigated at subgap photon energies. The results are described by a three-level generation-recombination model yielding the density of optically excitable trap states and additionally the ratio of optical to thermal cross sections.

The measurements were performed on polysilicon films of 380 nm thickness and an area of $10\times 20\,\mu m^2$, prepared by low-pressure chemical vapor deposition (LPCVD) in a self-aligning bipolar process. The polysilicon films were boron implanted with a dose of 5.0×10^{13} cm^{-2} at 40 keV, corresponding to a concentration of 1.3×10^{18} cm^3 acceptors. The films were deposited at 650 °C on a 310-nm-thick film of SiO_2, which was thermally grown on a lightly p-doped silicon wafer. Electrical contacts were formed by an additional boron implantation with a dose of 5.0×10^{15} cm^{-2}. Finally, the films were annealed and recrystallized at 950 °C for 8 min.

The samples were irradiated by a GaInAsP semiconductor laser at 1.3 μm wavelength, so that the corresponding photon energy is smaller than the gap energy. The photon flux density F was controlled by adjusting the current through the laser diode and monitored with a calibrated Ge photodiode. In Fig. 1 the measured photoconductance G of a typical sample is plotted versus the photon flux density F showing the essential result: for low photon intensities the photosignal increases superlinearly with F, and at about $F \geqslant 10^{18}$ cm^{-2} s^{-1} it starts to saturate.

Subgap photoconductivity can be understood in terms of the steady-state generation-recombination kinetics of free holes between the trap states in the grain boundary and the valence band. For a simplified description we assume the existence of uniformly sized grains and a shallow, simply ionized acceptor with concentration N_A. In the dark, localized states at the grain boundary are charged because of trapped holes down to the equilibrium Fermi energy level. This charge is compensated by ionized acceptors in a depletion layer on both sides of the boundary. The positive charge leads to an electrostatic potential barrier Φ_B, which controls the dark current density j_d according to

$$j_d \sim \exp(-e\Phi_B/k_b T)$$

(Ref. 11). Subgap photons excite trapped holes from the gap

Downloaded 18 Oct 2010 to 132.199.32.101. Redistribution subject to AIP license or copyright; see http://apl.aip.org/about/rights_and_permissions

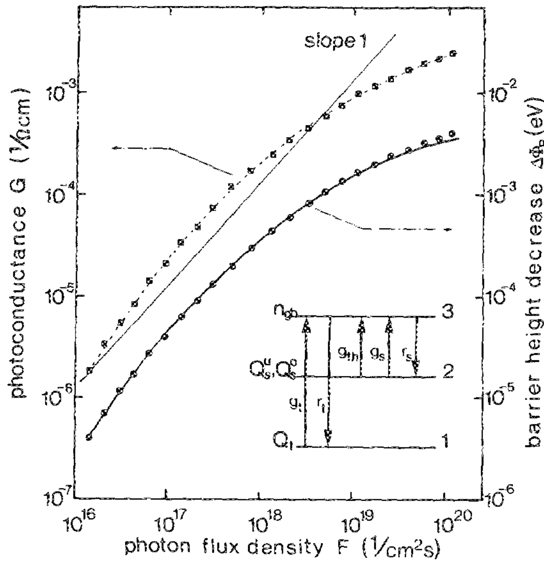

FIG. 1. Photoconductance G (left) and decrease of barrier height $\Delta\Phi_B$ (right) vs photon flux density F. The full line is a fitted curve, and the inset shows a schematic energy level diagram. For comparison, a straight line with slope one is drawn.

states to the valence band and reduce in this way the trapped charge density by ΔQ and the barrier height by $\Delta\Phi_B$. In low bias case the photocurrent is given by

$$j_{\rm ph} = j_d\,[\exp(e\Delta\Phi_B/k_bT) - 1]. \tag{1}$$

To describe the observed superlinear relation between photocurrent and photon flux, a kinetic model with at least three levels must be used as shown in the inset of Fig. 1. Each level is populated by one class of holes of equal physical characteristics. The lowest totally occupied level contains all optically excitable holes trapped below the Fermi energy. The first excited state represents the energy levels of the remaining localized states up to the band edge and level 3 is the valence band. Without illumination levels 1 and 2 are occupied by the total two-dimensional charge density Q_t and Q_s^0, respectively. The density of unoccupied states in level 2 is denoted by Q_s^u. For our model we consider separate detailed balance between the occupation of the valence band and that of level 1 and level 2, respectively. The charge density Q_t of the lowest level is determined by optical excitation g_t and thermal recombination r_t:

$$g_t = \sigma_{\rm opt}^t F(Q_t - \Delta Q_t),$$
$$r_t = v_{\rm th}\sigma_{\rm th}^t n_{gb}\exp(e\Delta\Phi_B/k_bT). \tag{2}$$

$\sigma_{\rm opt}^t$ and $\sigma_{\rm th}^t$ are the optical and the thermal cross sections, $v_{\rm th}$ is the thermal velocity, and n_{gb} is the concentration of free holes in the dark. ΔQ_t stands for the density of optical depleted states. As level 2 lies close to the valence band, additionally to the optical excitation g_s and to the thermal recombination r_s, the thermal excitation rate $g_{\rm th}$ has to be taken into account:

$$g_s = \sigma_{\rm opt}^s F(Q_s^0 + \Delta Q_s),$$
$$r_s = v_{\rm th}\sigma_{\rm th}^s n_{gb}\exp\left(\frac{e\Delta\Phi_B}{k_bT}\right)(Q_s^u - \Delta Q_s), \tag{3}$$

TABLE I. Trap densities Q_t, Q_s^0, and Q_s^u, and ratios of cross sections $\sigma_{\rm opt}^t/\sigma_{\rm th}^t$ and $\sigma_{\rm opt}^s/\sigma_{\rm th}^s$ obtained by fitting the experimental results with a three-level rate equation model.

$Q_t = (3.7 \pm 0.5)\times 10^{11}$ cm^{-2}
$Q_s^0 = (3.7 \pm 0.6)\times 10^{10}$ cm^{-2}
$Q_s^u = (2.4 \pm 0.6)\times 10^{10}$ cm^{-2}
$\frac{\sigma_{\rm opt}^t}{\sigma_{\rm th}^t} = (1.4 \pm 0.2)\times 10^{-2} v_{\rm th}$ s m^{-1}
$\frac{\sigma_{\rm opt}^s}{\sigma_{\rm th}^s} = (2.5 \pm 0.4)\times 10^{-3} v_{\rm th}$ s m^{-1}

$$g_{\rm th} = e_{\rm th}^s(Q_s^0 + \Delta Q_s).$$

ΔQ_s denotes an increase of the charge density Q_s^0, and $e_{\rm th}^s$ is the thermal emission rate into the valence band. The total decrease of charge density at the grain boundary under illumination ΔQ is the difference of ΔQ_t and ΔQ_s:

$$\Delta Q = \Delta Q_t - \Delta Q_s. \tag{4}$$

For the following calculation three assumptions are made: (i) parabolic band bending at the grain boundary, (ii) $\Delta\Phi_B \ll \Phi_B$, and (iii) $\Delta\Phi_B \ll k_bT/e$. Assumptions (ii) and (iii) are justified by the present experimental conditions and the application of relation (1). Assumption (i) is a commonly used approximation and is equivalent to

$$\Phi_B = e(Q_t + Q_s^0)^2/8\epsilon\epsilon_0 N_A, \tag{5}$$

where ϵ_0 is the vacuum permeability and ϵ is the dielectric constant of silicon. With Eq. (5) and assumption (ii), $\Delta\Phi_B$ is related to ΔQ according to

$$\Delta\Phi_B = \frac{e(Q_t + Q_s^0)}{4\epsilon\epsilon_0 N_A}\Delta Q. \tag{6}$$

Application of assumption (iii) allows us to replace the exponential term in the expressions for r_t and r_s by its linear approximation. Consideration of detailed balance gives

$$g_t = r_t \text{ and } g_s + g_{\rm th} = r_s. \tag{7}$$

Equations (7) together with (6) and (4) are an implicit expression for $\Delta\Phi_B$ as a function of the photon flux density F. By numerically fitting this expression to the measured values of $\Delta\Phi_B$, the unknown parameters Q_t, Q_s^0, Q_s^u, $\sigma_{\rm opt}^t/\sigma_{\rm th}^t$, and $\sigma_{\rm opt}^s/\sigma_{\rm th}^s$ are evaluated. The parameter set in Table I belongs to the fitted curve in Fig. 1. The points for $\Delta\Phi_B$ were calculated from the photocurrent according to Eq. (1). The fit is good except at the highest irradiation intensities. The reason for the deviation might be found in assumptions (ii) and (iii), which are only valid at low excitation rates. From the results listed in Table I, it is evident that the ratio of the optical to thermal cross section is distinctly smaller for states lying closer to the valence-band edge. The given ratios still depend on the thermal velocity $v_{\rm th}$. As the often-used saturation drift velocity $v_{\rm th} = 10^7$ cm s^{-1} (Ref. 9) is certainly far too high, we take $v_{\rm th}$ as parameter. The different ratios of the cross sections for the two energy levels may qualitatively be understood by the fact that the capture cross section of shallow impurities is larger than that of deeper lying levels. This shows that the assump-

Downloaded 18 Oct 2010 to 132.199.32.101. Redistribution subject to AIP license or copyright; see http://apl.aip.org/about/rights_and_permissions

tion of a constant ratio of the optical to thermal cross section across the whole band gap is not justified. The use of an average value for this ratio together with a constant σ_{opt} means that the capture cross section for shallower states will be underestimated and the corresponding density of states will be overestimated. On the other hand, the same assumption will lead to a far too small density of states around midgap. Thus a V-shaped distribution, as, e.g., reported in Refs. 6 and 7, will be flattened, approaching an U-shaped distribution if the decrease σ_{opt}/σ_{th} from midgap to the band edge is taken into account.

The densities of traps of level 2 are about one-sixth of that of level 1. The thermal activation energy $e\Phi_B$ for the samples was estimated to be about 170 meV by measuring the temperature dependence of the electrical resistance. Comparing $e\Phi_B$ with the gap energy, we find the same ratio as that of the unoccupied to occupied trap densities $Q_s^u/(Q_s^0 + Q_t)$. This suggests a nearly constant trap density over a wide range within the energy gap and does not allow a steep increase of the number of optically excitable traps towards the band edge. On the other hand, inserting Φ_B in Eq. (5) results in a total density N_{ss} of about 3.4×10^{12} cm^{-2}, which is nearly eight times as high as our fitted result. This shows that the larger fraction of traps is not optically excitable or has a very low optical cross section. Thus optical methods are not able to determine the absolute values of trap densities. The general validity of this result is confirmed by literature data. With optical methods[8,10] typical values for the density of about 10^{10}–10^{11} $cm^{-2}\,eV^{-1}$ were determined. In contrast, pure electrical methods[11] gave results up to 10^{14} $cm^{-2}\,eV^{-1}$ (normalized to a grain boundary thickness of 1 nm). Though the data of different workers cannot be directly compared, because the investigated samples were deposited, doped and post-treated in different ways, the generally smaller values obtained by optical experiments confirm our result.

In conclusion we showed that nonlinear subgap photoconductance in polysilicon yields details about the trap density at the inherent grain boundaries beyond previous investigations. Traps differ in their physical characteristics, especially in optical and thermal cross sections for excitation and recombination. Neglecting the variation of these parameters with respect to the energy level in the gap leads to an overestimation of the density near the band edge. Finally, we emphasized that traps are only by part accessible to optical excitations.

We thank L. Treitinger for helpful discussions. W. P. acknowledges financial support by the Deutsche Forschungsgemeinschaft.

[1]P. N. Panayotatos, in *Proceedings of Melecon, Mediterranean Electrochemical Conference, Athens 1983*, edited by E. N. Protontarios and G. I. Stassinopoulos, Athens, 1983, p. D802.1–D802.2.

[2]D. B. Meakin, P. A. Coxon, P. Migliorato, J. Stoemenos, and N. A. Economou, Appl. Phys. Lett. **50**, 1894 (1987).

[3]N. C.-C. Lu, L. Gerzberg, C.-Y. Lu, and J. D. Meindl, IEEE Trans. Electron Devices **ED-28**, 818 (1981).

[4]Y. W. Seto, J. Appl. Phys. **46**, 5247 (1975).

[5]N. C.-C. Lu, L. Gerzberg, C.-Y. Lu, and J. D. Meindl, IEEE Electron Device Lett. **EDL-2**, 95 (1981).

[6]J. Werner, M. Peisl, Phys. Rev. B **31**, 6881 (1985).

[7]S. Hirae, M. Hirose, and Y. Osaka, J. Appl. Phys. **51**, 1043 (1980).

[8]W. B. Jackson, N. M. Johnson, and D. K. Biegelsen, Appl. Phys. Lett. **43**, 195 (1983).

[9]C. Jacobori, C. Canali, G. Ottaviani, and A. Alberigi Quaranta, Solid-State Electron. **20**, 77 (1977).

[10]J. Werner, W. Jantsch, and H. J. Queisser, Solid State Commun. **42**, 415 (1982).

[11]G. E. Pike and C. H. Seager, J. Appl. Phys. **50**, 3414 (1979).

Downloaded 18 Oct 2010 to 132.199.32.101. Redistribution subject to AIP license or copyright; see http://apl.aip.org/about/rights_and_permissions